Acta Crystallographica Section F
Structural Biology and Crystallization Communications
ISSN 1744-3091

Cloning, overexpression, purification, crystallization and preliminary X-ray diffraction analysis of glyceraldehyde-3-phosphate dehydrogenase from *Antheraea mylitta*

Somnath Mukherjee, Samita Maity, Sobhan Roy, Suvankar Ghorai, Mrinmay Chakrabarti, Rachit Agarwal, Debajyoti Dutta, Ananta Kumar Ghosh* and Amit Kumar Das*

Department of Biotechnology, Indian Institute of Technology, Kharagpur 721302, India

Correspondence e-mail: aghosh@hijli.iitkgp.ernet.in, amitk@hijli.iitkgp.ernet.in

Received 6 July 2009
Accepted 13 August 2009

Glyceraldehyde-3-phosphate dehydrogenase from *Antheraea mylitta* (AmGAPDH) was cloned in pQE30 vector, overexpressed in *Escherichia coli* M15 (pREP4) cells and purified to homogeneity. The protein was crystallized using the hanging-drop vapour-diffusion method. The crystals belonged to the orthorhombic space group *I*222, with unit-cell parameters $a = 85.81$, $b = 133.72$, $c = 220.37$ Å. X-ray diffraction data were collected and processed to a maximum resolution of 2.2 Å. The presence of three molecules in the asymmetric unit gave a Matthews coefficient (V_M) of 2.80 Å^3 Da^{-1}, with a solvent content of 56.08%.

1. Introduction

The glycolytic pathway is the primary ATP-synthesizing pathway of the cell. The enzyme glyceraldehyde-3-phosphate dehydrogenase (GAPDH; EC 1.2.1.12) is the sixth enzyme of the glycolytic pathway. It acts on glyceraldehyde 3-phosphate (G3P) to convert it into 1,3-bisphosphoglycerate (1,3-BPG) and consumes inorganic phosphate to harness the energy into nicotinamide adenine dinucleotide (reduced) (NADH). The reaction takes place in two steps: an oxidoreduction reaction followed by phosphorylation of the thioester (Segal & Boyer, 1953; Trentham, 1971; Harris & Waters, 1976; Soukri *et al.*, 1989; Michels *et al.*, 1996; Talfournier *et al.*, 1998; Boschi-Muller & Branlant, 1999; Moras *et al.*, 1975). This glycolytic enzyme consists of two domains, a cofactor (NAD^+) binding domain and a catalytic domain, which have characteristic folds. The NAD^+-binding domain forms a compact substructure and has a characteristic Rossmann fold. The catalytic domain is an irregular S-shaped loop of amino-acid residues (178–201) and is involved in intersubunit interactions (Biesecker *et al.*, 1977). There are two phosphate-binding sites that accommodate the inorganic phosphate ion (P_i site) and the phosphate groups of G3P and 1,3-DPG (P_s site). The location of the P_s site in the three-dimensional structures of eukaryotic and bacterial GAPDHs is conserved and independent of the enzyme state (apo or holo form) and the presence of ligands such as sulfate ions, phosphate ions, substrate or substrate analogues. In contrast, the location of the P_i site appears to vary depending on the presence of ligands and the nature of the bound ligands or source organism (Moniot *et al.*, 2008).

Although the role of GAPDH as a housekeeping enzyme has been well investigated, recent investigations have revealed new properties of this enzyme arising from its localization on the cell surface, binding to cellular molecules and human A and B blood-group antigens (Pancholi & Fischetti, 1992; Gil-Navarro *et al.*, 1997; Delgado *et al.*, 2001; Gozalbo *et al.*, 1998; Zang *et al.*, 1998; Modun & Williams, 1999; Taylor & Heinrichs, 2002; Kinoshita *et al.*, 2008), and its involvement in apoptosis (Sirover, 1999).

Antheraea mylitta is an Indian non-mulberry Saturniidae silkworm, which is wild in nature and produces an exotic variety of silk called tasar silk, which is a widely popular textile material in India. In the present work, we report for the first time the cloning, overexpression, purification and preliminary X-ray diffraction analysis of GAPDH from the tasar silk-producing insect *A. mylitta*.

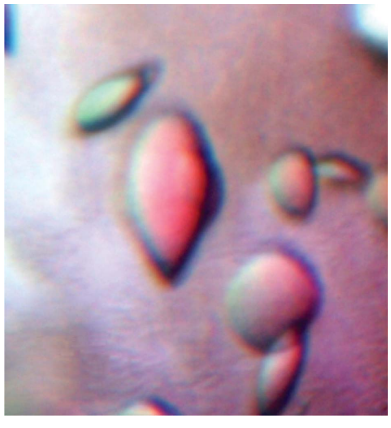

2. Methods

2.1. Cloning

The full-length cDNA clone (accession No. EG593014) encoding *A. mylitta* GAPDH was obtained by sequencing an EST library from the silk gland of fifth-instar larvae. The sequence corresponding to the open reading frame of GAPDH was amplified from GAPDH cDNA by PCR using the following primer pair: GAPDH F, 5′-ATATTCTAG**GGTACC**ATGTCGAAAATC-3′ (forward primer; *Kpn*I recognition site in bold), and GAPDH R, 5′-CAGAAA**CTG-CAG**TTAGTCCTTCGA-3′ (reverse primer; *Pst*I recognition site in bold). The amplicon (1029 bp) was digested with *Kpn*I and *Pst*I, cloned into the corresponding sites of bacterial expression vector pQE30 (Qiagen, USA) in frame with a sequence encoding six histidine residues at the N-terminus and transformed into chemically competent *Escherichia coli* XLBlue cells. The colonies were screened by restriction-enzyme digestion and the clones were verified by DNA sequencing. The positive clone of pQE30/GAPDH was transformed into *E. coli* M15 (pREP4) cells for overexpression of recombinant protein.

2.2. Overexpression and purification

The recombinant *E. coli* cells were grown in 1 l Luria broth with 100 µg ml^{-1} ampicillin and 25 µg ml^{-1} kanamycin at 310 K until the A_{600} reached 0.6 and were then induced with 1 m*M* IPTG and grown for a further 5 h. The cells were then harvested by centrifugation, resuspended in buffer *A* (10 m*M* Tris–HCl pH 8.0, 300 m*M* NaCl and 10 m*M* imidazole) containing a protease-inhibitor cocktail (0.1 m*M* each of leupeptin, pepstatin and aprotinin and 0.02 m*M* phenylmethylsulfonyl fluoride) and lysed by ultrasonication on ice; the supernatant was obtained by centrifugation at 20 000*g* for 40 min. The supernatant was loaded onto an Ni–NTA Sepharose High Performance affinity matrix (GE Healthcare) pre-equilibrated with buffer *A*. The column was then washed extensively with buffer *A* followed by buffer *B* (10 m*M* Tris–HCl pH 8.0, 300 m*M* NaCl and 20 m*M* imidazole) to remove bound contaminants. Finally, the bound protein was eluted with buffer *C* (10 m*M* Tris–HCl pH 8.0, 300 m*M* NaCl and 300 m*M* imidazole). Further purification was performed by size-exclusion chromatography using Superdex S-75 matrix in a 16/70C column (GE Healthcare) equilibrated with buffer *D* (10 m*M* Tris–HCl pH 8.0, 50 m*M* NaCl, 2 m*M* DTT) using an ÄKTAprime plus system (GE Healthcare). Fractions (2 ml) were collected at a flow rate of 1 ml min^{-1} and the peak fractions containing the desired protein were pooled together. The protein was obtained as a dimer after size-exclusion chromatography. The protein concentration was estimated by the method of Bradford (1976) and the purity was verified by 12% SDS–PAGE.

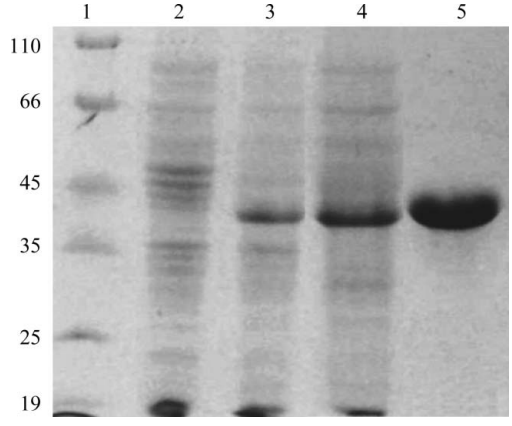

Figure 1
Analysis of recombinant AmGAPDH by 12% SDS–PAGE. Lane 1, molecular-weight markers (kDa); lane 2, uninduced *E. coli* lysate; lane 3, induced *E. coli* lysate; lane 4, supernatant of induced *E. coli* lysate; lane 5, AmGAPDH purified by Ni–NTA affinity and size-exclusion chromatography.

2.3. Crystallization

The purified protein was concentrated to 70 mg ml^{-1} using a 10 kDa cutoff Vivaspin 20 concentrator (GE Healthcare). Initial crystallization trials were performed by the sitting-drop vapour-diffusion method in a 96-well Corning CrystalEX microplate (Hampton Research). Droplets of 2 µl protein solution in buffer *D* were mixed with an equal volume of reservoir solution and equilibrated against 100 µl of the latter using commercially available sparse-matrix screens from Hampton Research (Crystal Screen and Crystal Screen II) at 298 K. Small crystals were obtained with (i) 0.1 *M* Tris–HCl pH 8.5, 2.0 *M* ammonium sulfate and (ii) 0.1 *M* HEPES pH 7.5, 1.4 *M* trisodium citrate. A fine screening around these conditions was performed varying the pH, ionic strength and precipitant concentration and using the hanging-drop vapour-diffusion method in 24-well Linbro plates. The crystallization experiments were carried out at 298 and 277 K. Plate-like crystals appeared overnight from 0.1 *M* HEPES pH 7.2, 1.2 *M* trisodium citrate and spindle-shaped crystals appeared from 0.1 *M* Tris–HCl pH 8.2, 1.8 *M* ammonium sulfate after 2 d at 298 K.

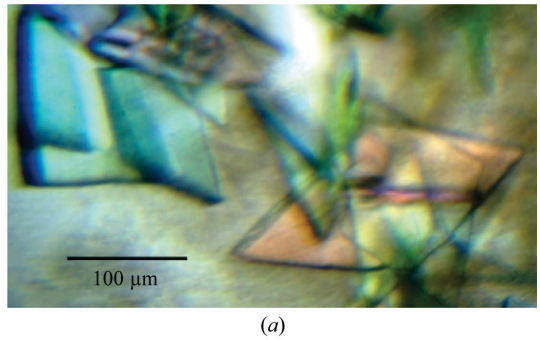

(*a*)

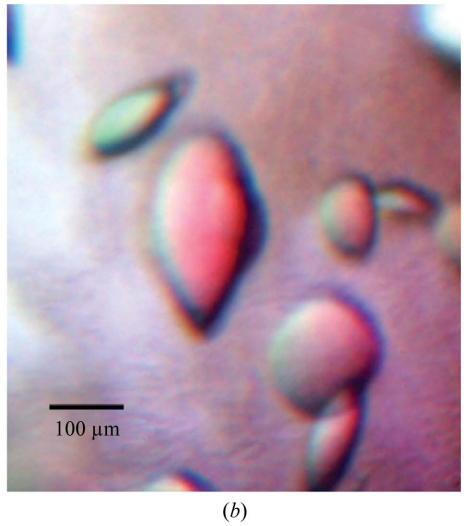

(*b*)

Figure 2
Crystals of AmGAPDH. (*a*) Typical crystals of AmGAPDH from 0.1 *M* HEPES pH 7.2, 1.4 *M* trisodium citrate at 298 K measured 0.20 × 0.12 × 0.04 mm; (*b*) those from 0.1 *M* Tris–HCl pH 8.2, 1.8 *M* ammonium sulfate at 277 K grew to typical dimensions of 0.2 × 0.09 × 0.02 mm.

Table 1
Data-collection and processing statistics.

Values in parentheses are for the highest resolution shell.

Wavelength (Å)	1.54
Space group	*I*222
Unit-cell parameters	
a (Å)	85.81
b (Å)	133.72
c (Å)	220.37
Unit-cell volume (Å^3)	2528714.693
Matthews coefficient (Å^3 Da^{-1})	2.80
Solvent content (%)	56.08
No. of molecules in ASU	3
Resolution range (Å)	27.03–2.20 (2.28–2.20)
Observed reflections	464286
Unique reflections	64506
Redundancy	7.20 (6.94)
Completeness (%)	99.9 (99.9)
$R_{\rm merge}$† (%)	7.9 (45.8)
Average $I/\sigma(I)$	10.2 (2.9)

† $R_{\rm merge} = \sum_{hkl}\sum_i |I_i(hkl) - \langle I(hkl)\rangle|/\sum_{hkl}\sum_i I_i(hkl)$, where $I_i(hkl)$ is the observed intensity of reflection *hkl* and $\langle I(hkl)\rangle$ is the mean intensity of reflection *hkl*.

2.4. Data collection

The diffraction data were collected using our home source (Cu $K\alpha$ X-rays generated by a Rigaku Micromax HF007 Microfocus rotating-anode X-ray generator equipped with a Rigaku R-AXIS IV^{++} detector and a Varimax mirror system and operated at 40 kV and 30 mA; Rigaku Americas Corporation). The cryoprotectant for the crystals obtained from 0.1 *M* HEPES pH 7.2, 1.2 *M* trisodium citrate was the reservoir solution; the crystals from 0.1 *M* Tris–HCl pH 8.2, 1.8 *M* ammonium sulfate were cryoprotected with 15% glycerol in the reservoir solution. The crystals were flash-cooled in a liquid-nitrogen stream at 100 K using a Rigaku X-stream 2000 cryosystem. The crystals obtained using trisodium citrate diffracted to a maximum of 5.5 Å resolution. The crystals from 0.1 *M* Tris–HCl pH 8.2, 1.8 *M* ammonium sulfate diffracted to a maximum resolution of 2.2 Å. Hence, data were collected over a 180° rotation range with an oscillation angle of 0.5° at 100 K using this crystal instead of the crystals that only diffracted to 5.5 Å. A total of 360 frames were collected with an exposure time of 2 min per frame and a crystal-to-detector distance of 150 mm. Diffraction data were processed with *d*TREK* v.9.8 software (Pflugrath, 1999).

3. Results and discussion

AmGAPDH was successfully cloned, expressed in *E. coli* and purified to homogeneity. The molecular weight of monomeric recombinant His$_6$-GAPDH (37.6 kDa) predicted from the sequence was confirmed by 12% SDS–PAGE (Fig. 1). The crystals obtained from 0.1 *M* HEPES pH 7.2, 1.4 *M* trisodium citrate at 298 K measured 0.20 × 0.12 × 0.04 mm (Fig. 2*a*) in size, while those obtained from 0.1 *M* Tris–HCl pH 8.2, 1.8 *M* ammonium sulfate at 277 K grew to typical dimensions of 0.2 × 0.09 × 0.02 mm (Fig. 2*b*). Diffraction data were collected using a cryoprotected single crystal obtained from 0.1 *M* Tris–HCl pH 8.2, 1.8 *M* ammonium sulfate. The crystal diffracted to a maximum of 2.2 Å resolution. Analysis of the symmetry and the systematic absences in the recorded diffraction patterns indicated that the crystals belonged to the orthorhombic space group $I222/I2_12_12_1$, with unit-cell parameters a = 85.81, b = 133.72, c = 220.37 Å. Determination of the Matthews coefficient suggested the presence of 56% solvent content in the unit cell ($V_{\rm M}$ = 2.80 Å^3 Da^{-1}) with three molecules in the asymmetric unit (Matthews, 1968). A total of 464 286 observed reflections were merged to 64 506 unique reflections in the 27.03–2.20 Å resolution range. The overall completeness of the data set was 99.9%, with an $R_{\rm merge}$ of 7.9%. The data-collection and processing statistics are given in Table 1. The structure was solved using the molecular-replacement method with the *MOLREP* program (Vagin & Teplyakov, 1997) within the *CCP*4 package (Collaborative Computational Project, Number 4, 1994). Because of its high sequence identity (79%) to AmGAPDH, human placental glyceraldehyde-3-phosphate dehydrogenase (PDB code 1u8f; Jenkins & Tanner, 2006) was used as the search model. A promising solution from *MOLREP* (correlation coefficient of 0.64) with three molecules in the asymmetric unit and interpretable electron density unambiguously ascertained the space group of the crystal to be *I*222. Similar results were obtained from *Auto-Rickshaw*, an automated crystal structure-determination pipeline (Panjikar *et al.*, 2005). The model obtained after molecular replacement was subsequently subjected to rigid-body refinement in *REFMAC*5 (Murshudov *et al.*, 1997) within the *CCP*4 package, giving an *R* factor of 34%. Final model building and restrained refinement using *REFMAC*5 are currently in progress. In parallel with the refinement, the preparation of crystals complexed with substrate and substrate analogues is in progress.

We thank the Director(s) of the Central Tasar Research and Training Institute and Ranchi and Jhargram for providing *A. mylitta* larvae. We are thankful to the Department of Biotechnology, India for providing the X-ray facility at IIT Kharagpur. SM and SR thank the Council of Scientific and Industrial Research for individual fellowships. The authors acknowledge the Department of Science and Technology, Government of India, Indian Council of Medical Research and IIT Kharagpur for financial assistance.

References

Biesecker, G., Harris, J. I., Thierry, J. C., Walker, J. E. & Wonacott, A. J. (1977). *Nature (London)*, **266**, 328–333.
Boschi-Muller, S. & Branlant, G. (1999). *Arch. Biochem. Biophys.* **363**, 259–266.
Bradford, M. M. (1976). *Anal. Biochem.* **72**, 248–254.
Collaborative Computational Project, Number 4 (1994). *Acta Cryst.* D**50**, 760–763.
Delgado, M. L., O'Connor, J. E., Azorin, I., Renau-Piqueras, J., Gil, M. L. & Gozalbo, D. (2001). *Microbiology*, **147**, 411–417.
Gil-Navarro, I., Gil, M. L., Casanova, M., O'Connor, J. E., Martinez, J. P. & Gozalbo, D. (1997). *J. Bacteriol.* **179**, 4992–4999.
Gozalbo, D., Gil-Navarro, I., Azorin, I., Renau-Piqueras, J., Martinez, J. P. & Gil, M. L. (1998). *Infect. Immun.* **66**, 2052–2059.
Harris, J. I. & Waters, M. (1976). *The Enzymes*, 3rd ed., edited by P. D. Boyer, ch. 13. New York: Academic Press.
Jenkins, J. L. & Tanner, J. J. (2006). *Acta Cryst.* D**62**, 290–301.
Kinoshita, H., Wakahara, N., Watanabe, M., Kawasaki, T., Matsuo, H., Kawai, Y., Kitazawa, H., Ohnuma, S., Miura, K., Horii, A. & Saito, T. (2008). *Res. Microbiol.* **159**, 685–691.
Matthews, B. W. (1968). *J. Mol. Biol.* **33**, 491–497.
Michels, S., Rogalska, E. & Branlant, G. (1996). *FEBS J.* **235**, 641–647.
Modun, B. & Williams, P. (1999). *Infect. Immun.* **67**, 1086–1092.
Moniot, S., Stefano, B., Vonrhein, C., Didierjean, C., Boschi-Muller, S., Vas, M., Bricogne, G., Branlant, G., Mozzarelli, A. & Corbier, C. (2008). *J. Biol. Chem.* **283**, 21693–21702.
Moras, D., Olsen, K. W., Sabesan, M. N., Buehner, M., Ford, G. C. & Rossmann, M. G. (1975). *J. Biol. Chem.* **250**, 9137–9162.
Murshudov, G. N., Vagin, A. A. & Dodson, E. J. (1997). *Acta Cryst.* D**53**, 240–255.
Pancholi, V. & Fischetti, V. A. (1992). *J. Exp. Med.* **176**, 415–426.
Panjikar, S., Parthasarathy, V., Lamzin, V. S., Weiss, M. S. & Tucker, P. A. (2005). *Acta Cryst.* D**61**, 449–457.
Pflugrath, J. W. (1999). *Acta Cryst.* D**55**, 1718–1725.
Segal, H. L. & Boyer, P. D. (1953). *J. Biol. Chem.* **204**, 265–281.
Sirover, M. A. (1999). *Biochim. Biophys. Acta*, **1432**, 159–184.

Soukri, A., Mougin, A., Corbier, C., Wonacott, A., Branlant, C. & Branlant, G. (1989). *Biochemistry*, **28**, 2586–2592.
Talfournier, F., Colloc'h, N., Mornon, J. P. & Branlant, G. (1998). *FEBS J.* **252**, 447–457.
Taylor, J. M. & Heinrichs, D. E. (2002). *Mol. Microbiol.* **43**, 1603–1614.
Trentham, D. R. (1971). *Biochem. J.* **122**, 59–69.
Vagin, A. & Teplyakov, A. (1997). *J. Appl. Cryst.* **30**, 1022–1025.
Zang, W. Q., Fieno, A. M., Grant, R. A. & Yen, T. S. (1998). *Virology*, **248**, 46–52.